Final laboratory results of visible nulling with dielectric plates

Rhonda M. Morgan[a], James H. Burge[b], and Neville Woolf[b]

[a]Jet Propulsion Laboratory, Pasadena, CA
[b]Steward Observatory,University of Arizona, Tucson, AZ

ABSTRACT

Nullng stellar interferometry may enable the discovery of earth-like planets around other stars. In nulling mode, the zero order fringe is destructive and on axis, thus cancelling light form a bright source and allowing detection of dimer off-axis features. To create a deep on-axis null, the phase must be shifted half a wave achromatically over a broad band. The phase shift is created by adding optical path thickness with dielectric plates. Plates of different materials can balance dispersion. The nulling solutions found for TPF (infrared) and SIM (visible)are promising.

This paper presents the final results of a dissertation that developed a nulling beam combiner testbed. The deepest null achieved over the spectral region of 600 to 800 nm was $7x10^{-3}$. The test bed revealed the extreme challenges of this technique and provided very valuable lessons to enable further implementations.

The testbed first achromatized the null by actively controlling the optical thicknesses of the plates. The phase as a function of wavelength was measured by PSI on a spectrally dispersed fringe. The phase was fit to a model to determine the optical thicknesses. The eigenfunctions of the model were nearly collinear and consequently the dynamic range required of the phase data was very high and not supported by the hardware. The testbed then searched for the null fringe and locked on the null using a 300 Hz servo loop and on a grey fringe. The OPD was stabilized to 6 nm peak-to valley.

Keywords: Nulling, dispersion, phase shifting interferometry, high dynamic range detection

1. INTRODUCTION

Nulling interferometry is a mode of interferometry in which the main, on-axis fringe is a destructive fringe, also called a null fringe. For quasi-monochromatic fringes, this is an uninteresting case, because the coherence envelope is so long that many orders of fringes can have high visibility. For broad band interferometry, the coherence envelope is short; the visibility deteriorates quickly away from the zero order fringe. In regular mode, the central, zero order fringe is constructive and the $\pm$ 1/2 orders are destructive, but not of great depth because of the quick deterioration of visibility. In nulling mode, the central, zero order fringe is destructive with a great depth, much deeper than the $\pm$ 1/2 orders of regular mode. Pictures of white light fringes in regular and nulling mode are shown in Figure 1 to illustrate the quick decline of visibility; a profile of the fringes shows that the zero order null of nulling mode is substantially deeper than the null depth of the $\pm$ 1/2 orders of regular mode. For broad band interferometry, a higher contrast is achieved in nulling mode than in regular mode. High contrast translates into the high dynamic range detection needed for the planet detection.

Planet detection re1quires high resolution and broad bandwidth. Nulling provides the high resolution as long as the phase shift is achromatic. It is difficult to create an achromatic phase shift because phase, which is some fraction of a wave, corresponds to a different physical optical path difference (OPD) for each wavelength. A half-wave of phase is 400 nm of OPD at λ = 800 nm, but 200 nm of OPD at λ = 400 nm. The phase shift is created by adding optical path thickness with dielectric plates. Plates of two different materials balance dispersion so that the phase shift is achromatic; this technique is not restricted to phase shifts of 180 degrees.

Send correspondence to Rhonda.M.Morgan@jpl.nasa.gov

Interferometry for Optical Astronomy II, Wesley A. Traub, Editor,
Proceedings of SPIE Vol. 4838 (2003) © 2003 SPIE · 0277-786X/03/$15.00

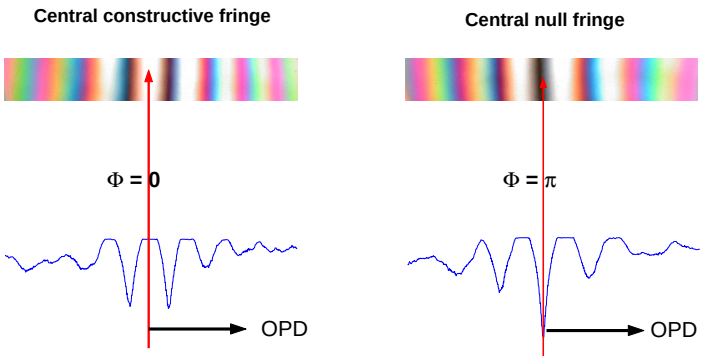

Figure 1. The left photo is normal white light interference fringes, the right is fringes in nulling mode. For the left image, the phase is zero at the central fringe (zero OPD). In nulling mode, the phase is half a wave at the zero OPD point. The plots of the logarithm of each fringe profile show that the null depth of nulling mode is much greater than the null depth of the ± 1/2 orders of constructive mode.

Nulling interferometer array configurations have been proposed that use $\lambda/2$, $\lambda/3$ and $\lambda/5$ phase shifts.[1] Optical path thickness is the only technique that can produce nulls at non-180 degrees and can be actively controlled to change phase in situ for on the fly array reconfiguration.

2. PHASE PLATES

White light interference fringes can be thought of as the superposition of monochromatic fringes at many wavelengths. The fringes are in phase at the zero OPD point and as OPD increases they become increasingly out of phase, decreasing in coherence (visibility).

A phase shift can be achieved by adding OPD, but with the penalty of decreased visibility. A phase shift can also be created by adding OPD with a dispersive medium. The material dispersion shifts each monochromatic fringe by a different amount according to its wavelength. The total effect, after summing the individually shifted fringes, is to shift the coherence envelope (change the group delay) and, for chromatic OPD changes, to change the shape of the coherence envelope.

2.1. Creating a Phase Shift while Balancing Wavelength

Let us consider the phase shift in a white light Michelson interferometer as optical thickness is incrementally added starting with vacuum path, then a single dielectric plate, and then a second dielectric plate.

To create a phase offset ϕ, the simplest option is to increase the optical path in one arm by moving an end mirror. The phase difference is now:

$$\phi(\lambda) = \frac{2\pi}{\lambda} s, \tag{1}$$

where s is the physical difference in path length through vacuum due to translating the mirror. The above phase term is linear with wavenumber. The resulting phase chromaticity is shown in Figure 2 for various values of s in the visible region for an octave of bandwidth. Any desired phase offset has a chromatic error.

We can balance the $1/\lambda$ term by adding optical thickness to the other arm of the interferometer. We can't add air: that would result in the original zero OPD. We can add optical thickness by adding glass or other dielectric optical material. The phase difference is then

$$\phi(\lambda) = \frac{2\pi}{\lambda}(s + n(\lambda)t), \tag{2}$$

where t is the glass thickness difference and $n(\lambda)$ is the index of refraction. The optical thickness is precisely balanced at one particular wavelength when $s = -n(\lambda_0)t$. The s and t can be selected to minimize the rms

phase error. The residual phase error is due to the nonlinear dispersion of the glass. The configuration and resulting chromaticity is illustrated in Figure 3. In the figure, the optical thickness is added by tilting the compensator plate so that the optical path through the compensator glass is longer.

We can balance this dispersion of the dispersion of a second glass or dielectric material. The two dielectrics are carefully selected to minimize the residual wavelength effects, just as with the glass selection for an achromatic lens. The three thicknesses (the vacuum path s and the two glass compensators $t_1 n_1(\lambda)$ and $t_2 n_2(\lambda)$) must be balanced to achieve the desired phase and to minimize the phase error. The phase difference is

$$\phi(\lambda) = \frac{2\pi}{\lambda} \left[s + n_1(\lambda) t_1 + n_2(\lambda) t_2 \right]. \tag{3}$$

The chromatic error can be reduced further by adding more plates of dielectric material.

The rms phase error versus bandwidth is plotted in Figure 5 for a natural null (using only vacuum spacing), for a single plate of material, and for two plates. We selected BK7 and silica for the visible and ZnSe and ZnS for the infrared. The bandwidth region is centered on 650 nm for the visible and 13 μm for the infrared. Infrared materials, whose dispersion is lower than visible materials, perform better at equivalent bandwidths. In the infrared, at two hundred percent bandwidth, a natural phase offset has an rms phase error of greater than 0.4 rads while two plates can yield nearly .001 rads. In the visible, two plates can yield .02 rads at two hundred percent bandwidth. The same rms phase as the infrared of .001 rads is achieved by two plates at a little less than one hundred percent bandwidth.

2.2. Particular Solutions

In the infrared, a fringe contrast of 10^{-6} is desired from 7 to 17 μm for the Terrestrial Planet Finder (TPF) mission.[2] This requires a phase error of less than .001 rads over more than an octave of bandwidth for a half wave phase shift.

The available infrared materials that transmit out to 17 μm are limited. All pair-wise combinations of the candidate materials were optimized for the deepest null. The materials and resulting null ratio are listed in Table 1. The combination of ZnSe with ZnS met the requirements, producing a null of less than 10^{-6} over the entire band, as shown in Figure 6.

Nulling was planned to be demonstrated in the visible, to the level of a 10^{-4} null at 20% bandwidth.[3] Our solution shown in Figure 6 uses BK7 and fused silica. Both materials have very low dispersions, very similar second order dispersion, but different indices of refraction. These glasses easily meet the requirements for a 10^{-4} null at 20% bandwidth. The requirement could still be met using the region from 440 nm to 920 nm, a bandwidth of 70%.

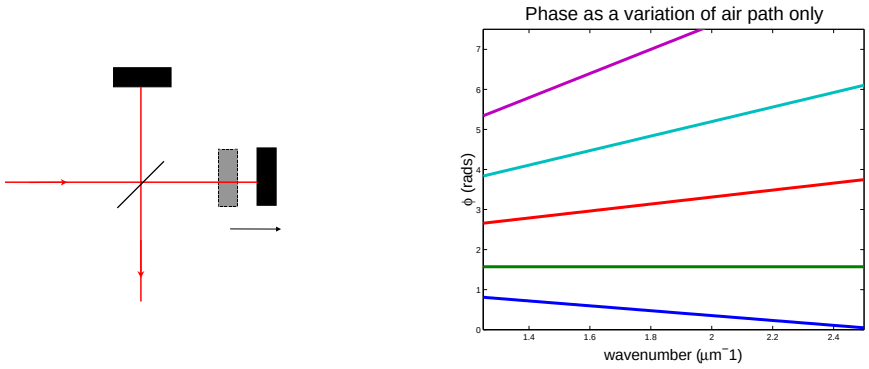

Figure 2. A phase shift can be created by translating one of the mirrors of the interferometer. This physical optical path difference corresponds to a different phase shift for each wavelength. The phase at various mirror spacings is plotted.

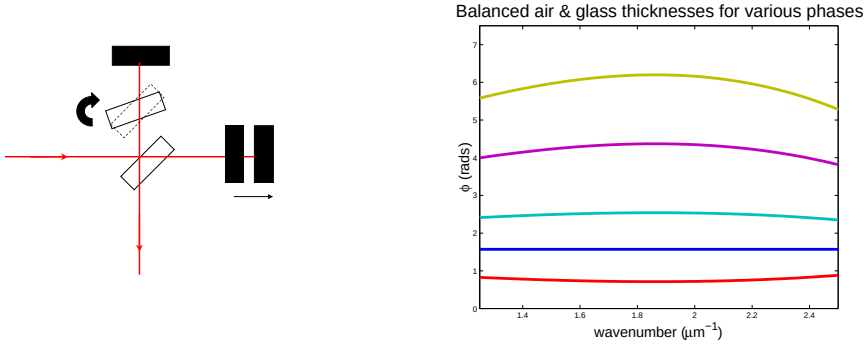

Figure 3. A phase shift is introduced by varying both the mirror translation and the tilt of the compensator plate. The linear phase error is balanced, leaving a residual error due to the nonlinear dispersion of the glass plate.

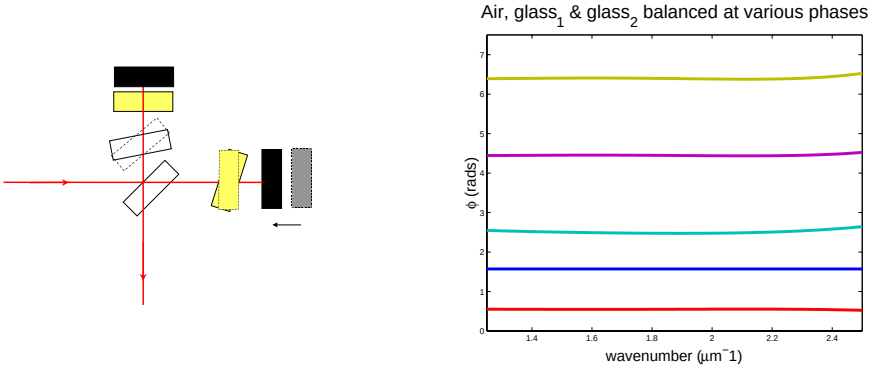

Figure 4. A second set of glass plates is added. A net phase shift is produced by balancing the tilts of the two types of plates and the mirror translation. Residual phase error is now third-order.

2.3. Controlling Optical Thicknesses

The precision required for visible nulling is very demanding. For the above SIM null, the plates are of thickness 1.9153 mm and 2.3453 mm with the tolerances of 45 nm. The required null can be met with a single plate of BK7 of thickness 8.98 μm with a vacuum spacing of -13.77 μm; the tolerance on the glass thickness is 1.2 μm. As these glass thicknesses are impractical to manufacture, a pair of plates of each glass is used whose thickness difference is t_1 or t_2; one plate is used as the beam splitter. These glass thickness tolerances are exceedingly difficult to achieve through manufacturing. But they can be attained by actively controlling the tilt of the plate. Increasing the tilt of the plate increases the optical path through the plate.

Active control of the glass plates is necessary to achieve the high precision nulls required for planet detection. Active control offers the ability to scan the central wavelength of the null to allow for interrogation of the spectra.

From a linear systems view, the input, or the control variables, are the optical thicknesses $\overrightarrow{t} = [s\, t_1\, t_2]$. The output is the phase as a vector over wavelength $\overrightarrow{\phi_\lambda}$. The phase plate system is described generally by

$$\overrightarrow{\phi} = \mathbf{H}\overrightarrow{t}, \tag{4}$$

where H is the system response function. The system matrix is derived by putting into matrix form the

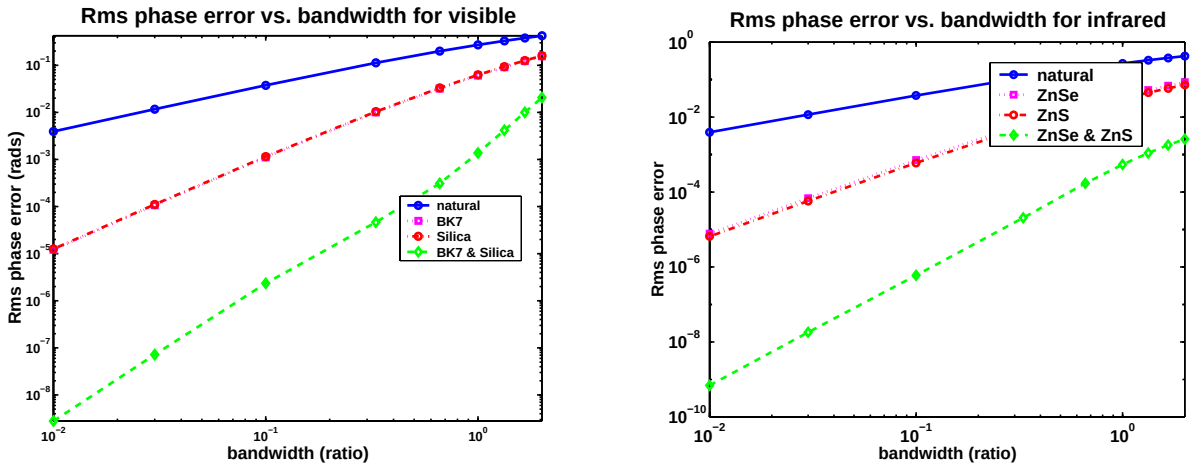

Figure 5. The rms phase error is plotted at various bandwidths for a phase shift produced by four optical path configurations: vacuum path alone (natural shift), a single plate balanced by vacuum OPD, a different single plate, and two plates balanced by vacuum OPD. The central wavelengths of the bandwidths were 650 nm and 13 μm.

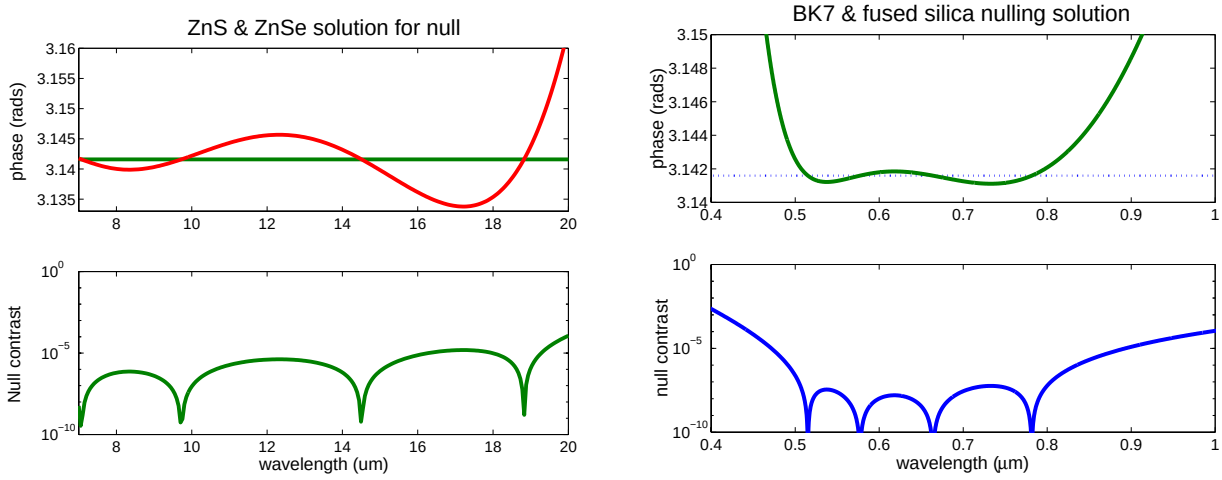

Figure 6. In the infrared from 7 to 17 μm, ZnS and ZnSe meets the TPF requirement of an rms null $< 10^{-6}$. In the visible spectrum, BK7 and fused silica can be balanced to produce a null that meets the SIM requirement of a null $< 10^{-4}$ over a 30% bandwidth in the visible. The null is $< 10^{-4}$ from 440 nm to 920 nm.

continuous equation 3 which describes the phase as a function of optical thickness and wavelength:

$$\begin{bmatrix} \varphi(\lambda_1) \\ \varphi(\lambda_2) \\ \vdots \\ \varphi(\lambda_i) \end{bmatrix} = 2\pi \begin{bmatrix} 1/\lambda_1 & n_1(\lambda_1)/\lambda_1 & n_2(\lambda_1)/\lambda_1 \\ 1/\lambda_2 & n_1(\lambda_2)/\lambda_2 & n_2(\lambda_2)/\lambda_2 \\ \vdots & & \\ 1/\lambda_i & n_1(\lambda_i)/\lambda_i & n_2(\lambda_i)/\lambda_i \end{bmatrix} \begin{bmatrix} s \\ t_1 \\ t_2 \end{bmatrix}. \tag{5}$$

The system matrix can be calculated theoretically from the properties of the dielectric materials or it may be measured empirically.

We can measure $\overrightarrow{\phi_\lambda}$ and find $\overrightarrow{t}$ using the inverse of the system response function:

$$\overrightarrow{t} = \mathbf{H}^{-1}\overrightarrow{\phi}. \tag{6}$$

Once the actual $\overrightarrow{t}$ is known, the thicknesses can be adjusted to the ideal $\overrightarrow{t_0}$ given by the above solution for the achromatized null.

2.4. Nonorgthogonality of Control Variables

A difficulty arises in controlling the achromaticity of the phase shift because the control variables are far from orthogonal; they are nearly colinear. This concept is illustrated in Figure 7 where $\widehat{s}$, $\widehat{t_1}$, and $\widehat{t_2}$ are basis vectors that point in nearly the same direction. If the basis set is orthogonalized, one vector is very long, one vector is very short, and one vector is very, very short. Adjusting only one input thickness adds offset and slope to the phase. A second input thickness must be adjusted to balance these first order effects until only the second order effects remain. When using two glasses, the second order effects must be balanced, requiring even greater precision. Consequently, the input variables must be balanced using large OPDs to high precision.

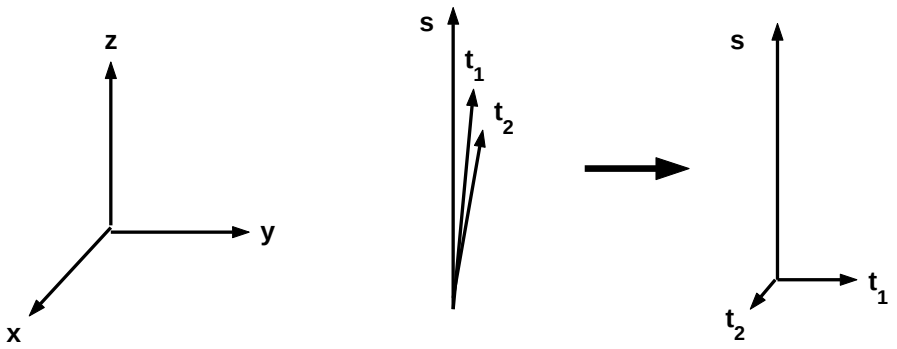

Figure 7. An ideal system has orthogonal eigenfunctions, as seen on the left. The input variables of the phase plate system are nearly colinear (middle). Transformed into orthogonal eigenfunctions, their vector lengths vary substantially (right).

This concept is quantified by examining the Singular Value Decomposition (SVD) of the system matrix. The SVD finds the eigenfunctions and eigenvalues of the system matrix.[4] In order to resolve the smallest eigenfunction $\widehat{t_2}$, the data must have a dynamic range, at the least, calculated by dividing the smallest eigenvalue into the largest eigenvalue.

For the two-plate, ZnS/ZnSe solution for TPF from 7 to 17 μm, the ratio of smallest to largest eigenvalues, and thus the required dynamic range of the phase data is $1.06\text{x}10^4$. The same dynamic range is required for the two plate BK7/silica solution in the visible band pass of 600 nm to 800 nm. A single plate of BK7 can provide a 10^{-4} null in the 600-800 nm pass band and a dynamic range of $2.06\text{x}10^3$ is required.

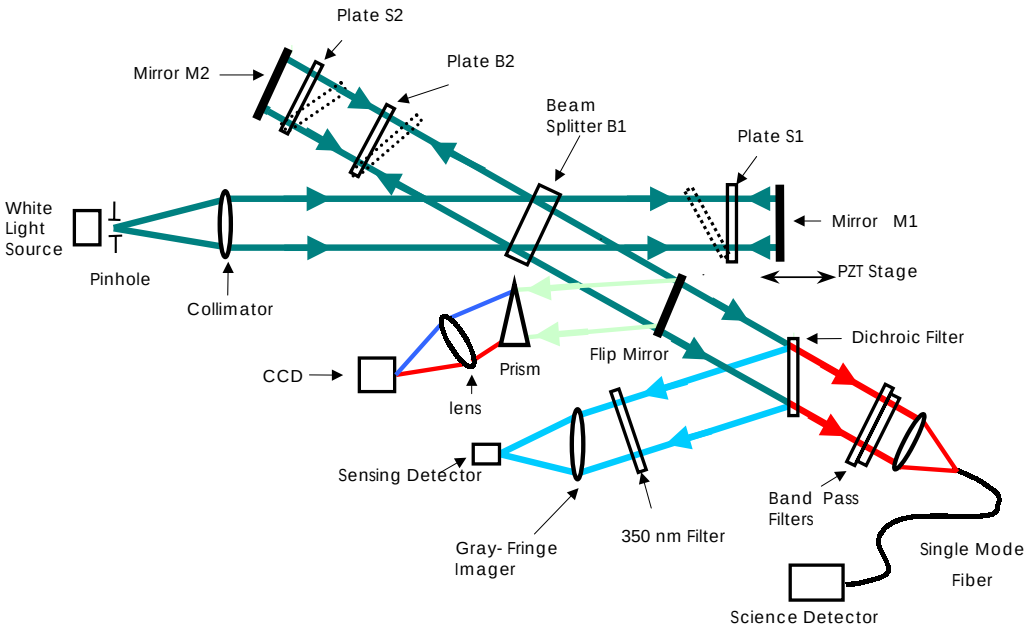

Figure 8. Experimental layout of the white light nulling interferometer. The output is spatially filter by a single mode fiber and detected by a PMT. A photodetector senses the grey fringe for the stabilizing servo loop. The branch with the prism and CCD measures $\phi(\lambda)$

3. NULLING BEAM COMBINER TESTBED

An infrared, planet-detecting beam combiner requires nm level phase control and 0.1% amplitude control. A phase error of 1 nm in the visible corresponds to a null of 10^{-4} and requires amplitudes to be equal to 4%, achievable without active amplitude control.

The laboratory testbed is implemented as a white light Michelson style interferometer as in figure 8. Because a Michelson is a double pass interferometer, the two arms have equal amplitudes, and the phase control issue can be addressed without simultaneously addressing amplitude control. A single mode fiber spatially filters the output to eliminate the background irradiance due to surface scatter and irregularity.

The system is composed of three tiers of control. The first tier tilts the plates to perform the achromatization. The second tier sweeps through the white light fringe to record the peak irradiance and to locate the null. The third tier is a fast servo loop that stabilizes the null. Each tier operates over different time scales. Tier 1 controls chromaticity by tilting optical plates and is a static control loop. Tier 2 searches for the null as the air path drifts over minutes. Tier 3 stabilizes the null at a 300 hertz rate.

3.1. Achromatize the Null

The phase is measured using phase shift interferometry (PSI) techniques. The fringe is spectrally dispersed and imaged on a CCD. The OPD in air is incremented in 4 equal steps while a sequence of frames are captured. The sequence of 4 frames are reduced by the Carré algorithm. The Carré algorithm allows for OPD increments

Table 1. Infrared materials were evaluated in pairs to create a null fringe. The table gives the normalized irradiance of the null fringe multiplied by 10^6 for a band width from 7 to 17 μm.

Material	CdSe	CdTe	CsBr	CsI	Ge	KBr	KCl	KRS5	ZnS	ZnSe
AgCl	82	29	11	0.9	3	49	15	4	15	75
CdSe		149	545	106	20	91	54	69	32	79
CdTe			91	186	10	40	16	397	3	6
CsBr				11	5	5	12	22	13	33
CsI					2	1.3	2	37	5	9
Ge						5	2	1.7	194	33
KBr							23	7	17	69
KCl								1.7	15	311
KRS5									1.1	1.7
ZnS										0.7

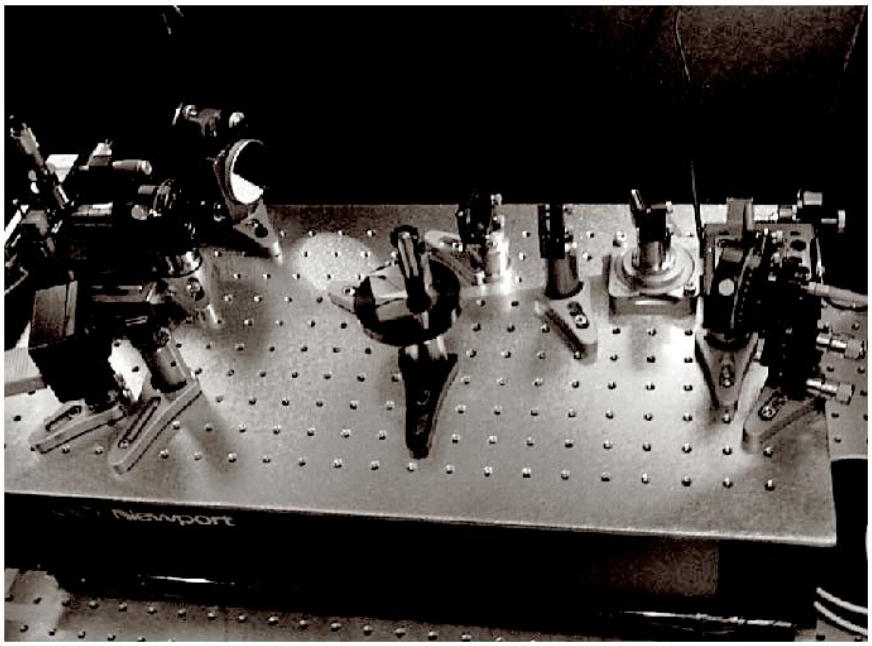

Figure 9. The interferometer was constructed on a small floating optical bench on a larger floating optical table to minimize vibration. Most optics are 0.5 inches in diameter. The interferometer has a small beam and short arms to minimize air turbulence effects.

that are non-90 degrees and not known. The physical OPD step translates into a different increment of phase for each wavelength.

The phase measured by the PSI process is known relatively, not absolutely. The absolute phase is an integer multiple of 2π added on to the relative phase. The absolute phase must be included as one of the parameters of the fit for the optical thicknesses. The behavior of the chromaticity of the phase was studied by varying the

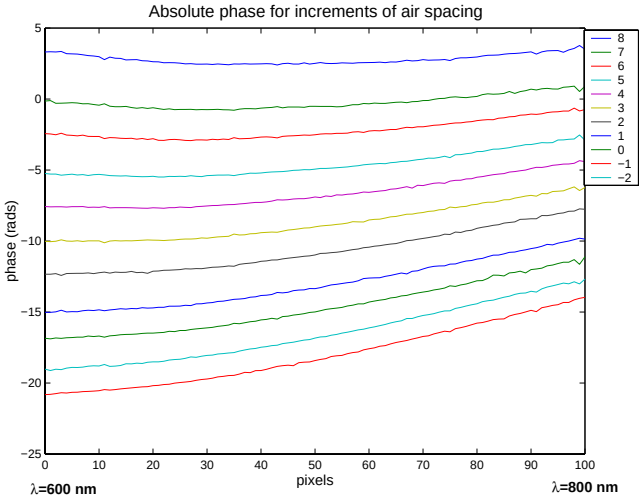

Figure 10. The phase was measured for 320 nm increments of OPD in air.

OPD in air as shown in Figure 10 and the OPD in glass. A systematic dispersion was observed. The dispersion was attributed to a dielectric anti-reflection coating. The dispersion of the coating was included in the system model and balanced by the other dielectric materials in the system. The dynamic range required of the phase data then becomes on the order of 10^4, the same as for a dual plate solution. The coating dispersion, if balanced by BK7 dispersion, would limit the null to $1.1\text{x}10^{-3}$. To reach this null, the BK7 OPD must be 56.7 μm $\pm$60 nm. The OPD tolerance translates into a tolerance of plate tilt angle of 14 arcseconds. The rotation stage only had a resolution of 40 arcseconds which could limit the null to 0.14.

3.2. Locate the Null

The white light fringe is scanned. This provides a quick estimate of the null depth as a check of the Tier 1 achromatization and allows selection of the correct null. The PZT is scanned through 10 fringes (about 20 μm) while the fringe irradiance is read out on the science channel, which is a hybrid solid state channel photomultiplier (CPM). The fringe scan is inspected for symmetry and the deepest fringe selected as the null. The PZT location at the deepest fringe is used as the starting point of the fine resolution null search.

The PZT is dithered a fraction of a wave over the null while the CPM is read. The dither data is averaged and fit by least squares to a parabola as an approximation of the bottom of the cosine fringe. The center of the parabola is set as the calibrated null position.

Figure 11 shows a laser null with contrast ratio of $9.1\text{x}10^{-4}$. The CPM is saturated by the peak of the fringe, so the physical null is greater but the CPM was limited to this measurement. A laser null of $1.04\text{x}10^{-4}$ has been measured previously with a photodiode and manual PZT control.[5]

3.3. Stabilize the Null

Tier 3 stabilizes the null in the presence of vibrations and air turbulence. The output of the interferometer, before entering the single mode fiber, encounters a dichroic beamsplitter. Wavelengths shorter than 450 nm are reflected to a photodiode while the longer wavelengths of the main passband, 600 to 800 nm, transmit through the dichroic beamsplitter, couple into a single mode fiber and are detected by the CPM. At the shorter

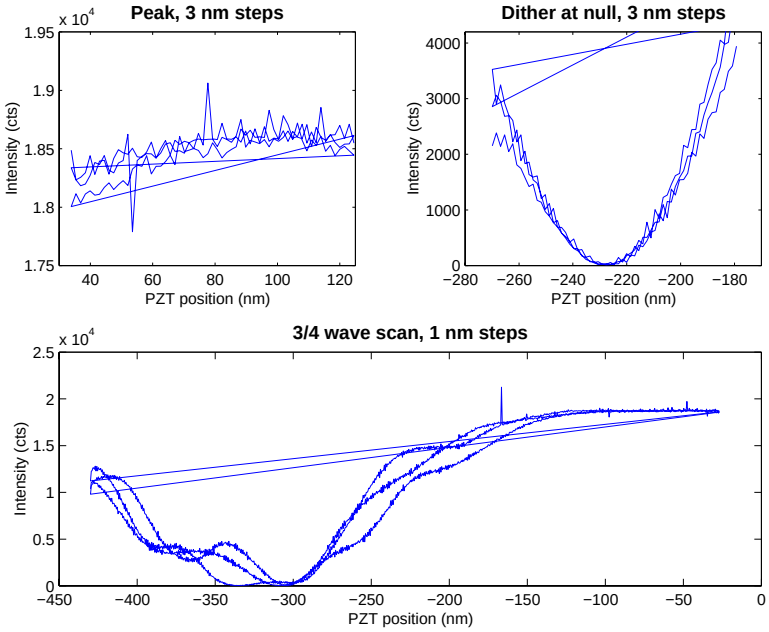

Figure 11. A laser was used to produce high contrast fringes. The PZT was scanned over 270 nm of OPD in 3 nm increments to finely sample the peak (top left) and the null (top right). A full fringe scan with 1 nm sampling took 36 seconds and was disturbed by air motion (bottom).

wavelength, the fringe phase is grey when the main band pass fringe is a null. The OPD is stabilized on the grey fringe intensity detected by the photodiode.

The photodiode is read with 12 bit analog to digital (A/D) converter. A proportional-derivative servo control loop, implemented in software, locks onto the desired grey fringe light level. The control loop moves the PZT as necessary to maintain the grey fringe light level.

The low voltage PZT translation stage is operated with a -10 to 10 Volt, 16 bit digital to analog (D/A) converter. The measured translation is 1 Volt produces a mean of 185 nm of translation, with standard deviation .8 nm. The smallest resolution expected with the 16 bit D/A driver is 0.3 nm, which is below the standard deviation of the calibration. Achieving 1 nm resolution with the PZT stage is the best expected performance.

The light reflected from the dichroic was very faint, in the 10 mV regime at peak fringe. An amplifier with gain of 1000 was used but limited the signal to noise ratio to 10.3. This was insufficient to stabilize a white light null with depth greater than ten. The servo loop performed successfully on a high signal laser null. Shown in Figure 12, the OPD is stabilized to 6nm peak to valley.

4. MEASURED WHITE LIGHT NULLS

Scans through nulls for various bandwidths were measured. The null was found by manually adjusting the plate tilt until the fringe was symmetric about the null. The fringe was then visually examined to verify that the central null was black and that the fringe colors were symmetric about the null.

The fringe intensity was acquired on the CPM while the PZT scanned the OPD repeatedly through 4.8 μm and then averaged to produce the nulled, broad band fringes shown in Figure 13. The OPD step resolution was 40 nm which could, in a worst sampling case, limit a monochromatic null to 0.033. The integration time for each sample was 30 msec for 600-800 and 600-700 nm, 20 msec for 600-650 nm, and 10 msec for the broadest band pass. The null contrast ratio for each band pass is given in Table 2.

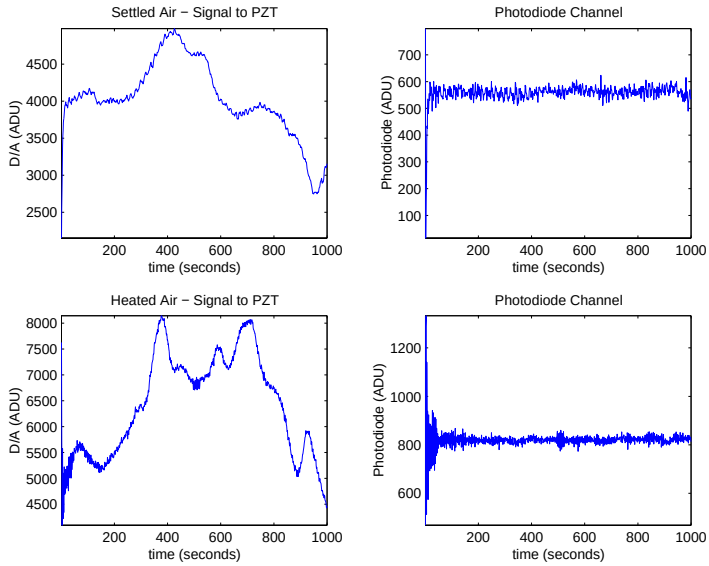

Figure 12. A laser provides a strong signal to the sensing channel. The control signal sent to the PZT (top left plot) reveals the environmental noise that was overcome to provide the stable signal on the photodiode (top right plot). The bottom two plots show the control signal and the stabilized signal in the presence of air turbulence.

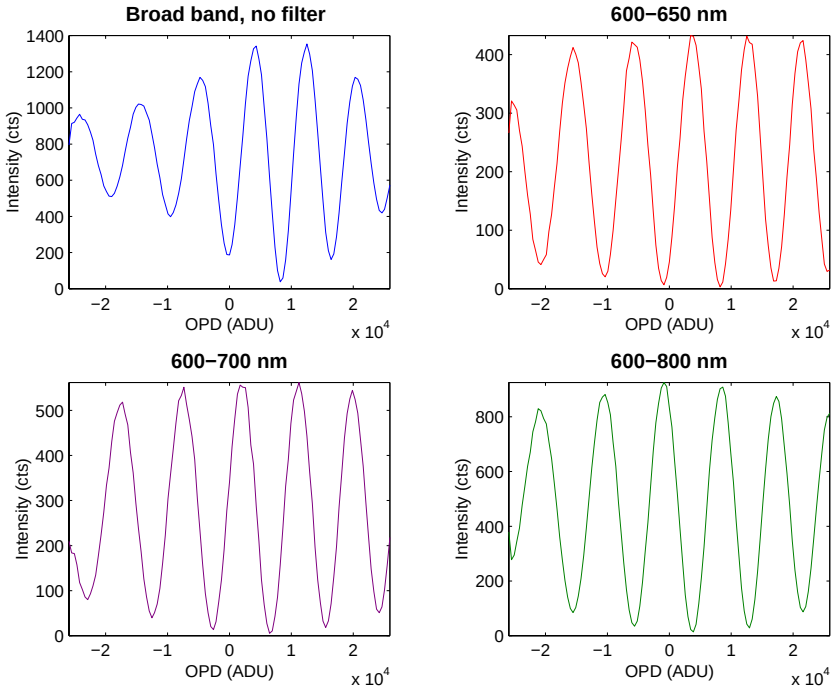

Figure 13. The nulled fringe was scanned over 8 waves of OPD for various band passes: 600-650 nm (upper right), 600-700 nm (lower left), 600-800 nm (lower right). In the upper left plot, no filter was used.

Table 2. The nulled, broad band fringes were measured for various band widths. The null contrast ratios were calculated from the data presented in Figure 13.

band pass	null ratio
no filter	0.028
600 - 800 nm	0.0069
600 - 700 nm	0.009
600 - 650 nm	0.015

5. CONCLUSION

The beam combiner testbed performed several unique feats. The first was to phase shift on a dispersed fringe and reduce the data with the Carré algorithm. The behavior of the chromaticity of the phase was studied by varying the OPD in air and the OPD in glass. OPD control by sensing on a grey fringe pass band was demonstrated to 6 nm peak-to-valley.

A possible future implementation is a nulling beam combiner in the infrared to demonstrate a 10^{-6} null. Such an infrared testbed could be directly built from the lessons of this visible testbed without finalizing the 10^{-4} visible null. However, the infrared beam combiner for such a deep null will require active amplitude control, which should perhaps first be developed in its own testbed.

ACKNOWLEDGMENTS

This work was performed at the University of Arizona and supported by NASA Graduate Student Research Program award NGT5-50046 and grant # 961286 from the California Institute of Technology's Jet Propulsion Laboratory, operated under contract to NASA.

The authors benefited from the insights and advice of Jim Breckenridge, Stuart Shaklan, Bill Hoffman, Roger Angel, Michael Lloyd-Hart, Don McCarthy, and Derek Sabatke. Rigel Woida, Kameron Rausch, Matt Cheselka, and Brian Duffy provided lab assistance.

REFERENCES

1. B. Menesson and J.-M. Mariotti, "Array configurations for a space infrared nulling interferometer dedicated to the search for earthlike extrasolar planets," *Icarus* **128**, pp. 202–212, 1997.
2. C. Beichman, N. Woolf, and C. Lindensmith, *The Terrestrial Planet Finder (TPF): A NASA Origins Program to Search for Habitable Planets*, NASA JPL, Pasadena, 1999.
3. D. Peterson and M. Shao, *Space Interferometry Mission (SIM): Taking Measure of the Universe*, NASA JPL, Pasadena, 1999.
4. H. Barrett and K. Myers, *Fundamentals of Image Science*, Wiley and Sons, in press, 2002.
5. R. Morgan and J. Burge, "Initial results of a white light nulled fringe," in *Interferometry in Optical Astronomy*, P. Lena and A. Quirrenbach, eds., *Proc. SPIE* **4006**, 2000.